ELSEVIER

# Synthesis of molybdenum silicide by both ion implantation and ion beam assisted deposition

Qingli Meng [a], Jizhong Zhang [a,b,*], Zhanping Li [c], Gaobao Li [a], Runbing Chen [d]

[a] *Laboratory of Advanced Materials, Department of Materials Science and Engineering, Tsinghua University, Beijing 100084, China*
[b] *International Centre for Materials Physics, Chinese Academy of Sciences, Shenyang 110016, China*
[c] *Analysis Center, Tsinghua University, Beijing 100084, China*
[d] *Baotou Iron & steel (group) Co., Ltd., Baotou 014010, China*

## Abstract

Two groups of Mo/Si films were deposited on surface of Si(1 0 0) crystal. The first group of the samples was prepared by both ion beam assisted deposition (IBAD) and metal vapor vacuum arc (MEVVA) ion implantation technologies under temperatures from 200 to 400 °C. The deposited species of IBAD were Mo and Si, and different sputtering Ar ion densities were selected. The mixed Mo/Si films were implanted by Mo ion with energy of 94 keV, and fluence of Mo ion was $5 \times 10^{16}$ ions/cm$^2$. The second group of the samples was prepared only by IBAD under the same test temperature range. The Mo/Si samples were analyzed by X-ray diffraction (XRD), atomic force microscopy (AFM), scanning electron microscopy (SEM), X-ray photoelectron spectroscopy (XPS), sheet resistance, nanohardness, and modulus of the Mo/Si films were also measured. For the Mo/Si films implanted with Mo ion, XRD results indicate that phase of the Mo/Si films prepared at 400 and 300 °C was pure MoSi$_2$. Sheet resistance of the Mo/Si films implanted with Mo ion was less than that of the Mo/Si films prepared without ion implantation. Nanohardness and modulus of the Mo/Si films were obviously affected by test parameters.
© 2007 Elsevier B.V. All rights reserved.

## 1. Introduction

Nowadays more and more multilayer films were applied in coating technology to improve the surface properties of devices [1]. Molybdenum disilicide (MoSi$_2$) is considered to be a promising high temperature material for turbojet and hypersonic engines in aerospace and various industrial applications, because of a high melting point (2030 °C), adequate density (6.3 g/cm$^3$), and an excellent oxidation resistance [2]. The sliding friction and wear properties of intermetallic MoSi$_2$ film are good, and they are used in many aspects. The mechanical durability of thin film is of much importance for coated products, and is well-known to be influenced by mechanical and tribological properties of thin film [3–5].

In ultra-large-scale-integrated (ULSI) circuit application and other fields, silicon plays an important role as substrate material [6]. Molybdenum disilicide (MoSi$_2$) intermetallics possesses good electrical property. As technology of the mobile phone and laptop developing, MoSi$_2$ is widely used in the field of micro-electronics in order to get smaller electric apparatus. For example, MoSi$_2$ is an important material to produce grid of ultra-large-scale-integrated circuit. Also, MoSi$_2$ is used in industry to produce electric cooker, high temperature heat exchanger, and some parts of turboengine of automobile [7].

So far several methods to deposit a layer of MoSi$_2$ film on Si substrate have been reported, such as chemical vapor deposition (CVD), physical vapor deposition (PVD), electrochemical deposition, etc. [8,9]. Ion beam assisted deposition (IBAD) is a method of thin film deposition which can produce compact and uniform thin films at low temperatures [10]. Metal vapor

* Corresponding author at: Laboratory of Advanced Materials, Department of Materials Science and Engineering, Tsinghua University, Beijing 100084, China. Tel.: +86 10 6277 1809; fax: +86 10 6277 1160.
   *E-mail address:* zjz@mail.tsinghua.edu.cn (J. Zhang).

vacuum arc (MEVVA) is widely used in improving properties of surface of materials [11]. Combining IBAD technology and MEVVA ion implantation technology is of many advantages. They are used to provide preferable bonding between the deposited film and substrate [12,13]. In this paper, structure and properties of the $MoSi_2$ films prepared by both IBAD and MEVVA ion implantation technologies were reported.

## 2. Experimental

N-type single crystal Si(1 0 0) wafer of 435 μm in thickness with a resistivity of 5.5 Ω cm was used in the experiment. The N-type Si(1 0 0) wafer was cut into the pieces with size of 10 mm × 10 mm, numbered A, a, B, b, C and c, respectively. They were ultrasonically cleaned with acetone and alcohol, respectively, then, rinsed with de-ionized water. The schematic drawing of the MEVVA–IBAD devices is shown in Fig. 1. The base pressure of the vacuum chamber was better than $5 \times 10^{-4}$ Pa. Prior to test, argon ions were irradiated on surface of the Si substrate firstly at a voltage of 20 kV with an ion density of 0.02 mA/cm$^2$ for 10 min, then at a voltage of 4 kV with an ion density of 0.02 mA/cm$^2$ for 20 min by using medium energy ion source to clean away oxide and impurity.

For the first group of samples, preparation of the Mo/Si films included both deposition and implantation. Firstly, molybdenum and silicon were deposited simultaneously on surface of the silicon substrate by IBAD. The voltage of sputtering Ar ion beam was 2.75 kV for both Mo target and Si target, and current of the sputtering Ar ion beam for Mo target was 20 mA and one for Si target was 100 mA. During each deposition process,
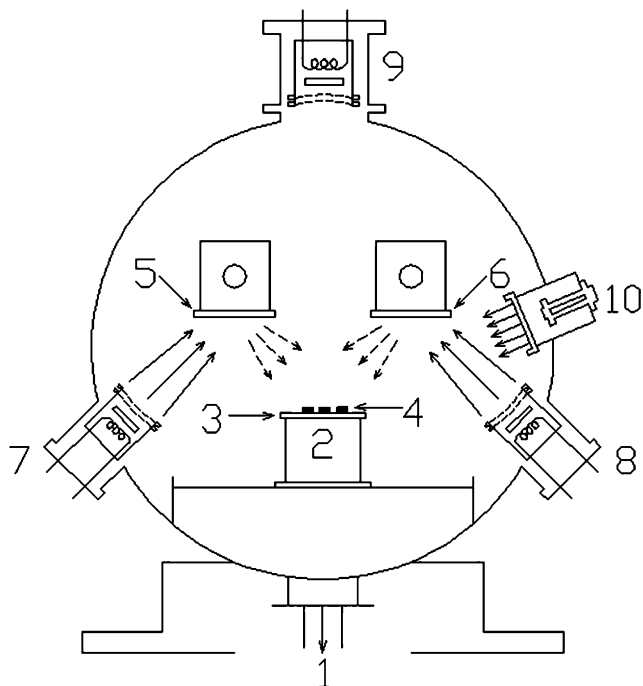


Fig. 1. Configuration of the MEVVA–IBAD device used in the work. 1: Jointed with molecular pump; 2: heating system; 3: sample holder; 4: samples; 5: Mo target; 6: silicon target; 7: low-energy Kaufman ion source; 8: low-energy Kaufman ion source; 9: medium-energy Kaufman ion source; 10: MEVVA ion source.

thickness of the Mo/Si mixing film was controlled at 30 nm. After each IBAD deposition, molybdenum ions were implanted into the Mo/Si mixing film at a fluence of $5 \times 10^{16}$ ions/cm$^2$ by using a MEVVA ion implanter at a voltage of 40 kV. The mean charge state of molybdenum ion was $Q_p = 2.35$, therefore, the energy of molybdenum ion was 94 keV. The projected rage of Mo ion with energy of 94 keV into Si is 55 nm, and the projected rage of the same Mo ion into Mo is 20 nm, which were calculated by TRIM code [14]. It means that during each implantation process, each Mo ion can completely penetrate through the Mo/Si mixing film. After Mo ion implantation, the second deposition of Mo and Si on surface of the first layer of Mo/Si mixing film was carried out. In the experiment, the deposition–implantation process was repeated for six times.

For the second group of the samples, the Mo/Si films were prepared only by IBAD without any Mo ion implantation. Molybdenum and silicon were deposited simultaneously on surface of the silicon substrate. The parameters of IBAD used in preparing the second group of the samples were the same as those in preparing the first group of the samples. Thickness of the Mo/Si mixing films were controlled around 180 nm.

During the experiment, the test temperature of Si substrate was keep at 400 °C for A group of the samples (including 'A' series and 'a' series), at 300 °C for B group of the samples, and at 200 °C for C group of the samples. Both B group and C group have the same sample numbering method as one of A group of the samples. Preparation parameters of all the samples are shown in Table 1.

X-ray diffraction (XRD) was employed to identify phase of the samples. SEM, JSM-6460LV, was used to observe morphology of the samples. AFM was used to characterize morphology and root mean square (RMS) roughness of the samples. XPS was used to analyze chemical bonding and to compare the relative amount of different components in the films. A surface topography device, Talysurf 5P-120, UK, was employed to measure thickness of the samples. Four-probe instrument, model D41-5/2M, Seven-star, was used to measure sheet resistance of the samples. XP nano-indenter, MTS, USA, was employed to measure nanohardness and modulus of the samples.

## 3. Results and discussions

### 3.1. Morphology and thickness of the Mo/Si films

Morphologies of the Mo/Si films were observed by SEM. It is clear from Fig. 2(a–d) that under the same test temperature, the as-implanted Mo/Si films were not as smooth as the non-implanted Mo/Si films. It can be explained that Mo ion implantation resulted in much rough surface because of irradiation damage. Compare to morphology of the samples A, a, B, and b, surfaces of the samples C and c were smoother (not shown here). It indicates that influence of the test temperature to surface smooth of the Mo/Si film was positive.

Thickness values of the Mo/Si films are listed in Table 2. It can be seen that the thickness values of all the samples were very close. The thickness of the samples a, b and c are almost

Table 1
Preparation parameters of all the Mo/Si films

| Process | Temperature (°C) | IBAD | | | MEVVA |
|---------|------------------|------|---|---|-------|
| Sample no. | | Sputtering Ar ion current (mA) | | Deposition time (min) | Ion implantation |
| A | 400 | Mo (20) | Si(1 0 0) | 6 | Done |
| a | 400 | Mo (20) | Si(1 0 0) | 6 | – |
| B | 300 | Mo (20) | Si(1 0 0) | 6 | Done |
| b | 300 | Mo (20) | Si(1 0 0) | 6 | – |
| C | 200 | Mo (20) | Si(1 0 0) | 6 | Done |
| c | 200 | Mo (20) | Si(1 0 0) | 6 | – |

the same as one of the samples A, B and C, respectively. It means that fluence of the implanted Mo ion was only $5.0 \times 10^{16}$ ion/cm$^2$, and did not change thickness of the deposited Mo/Si film.

The root mean square (RMS) roughness of the Mo/Si films was tested by AFM. Fig. 3 shows AFM images of the samples A, a, B, and b. The AFM images shown in Fig. 3(b and d) are not clear enough due to smoother surfaces of both the sample a and sample b. The RMS roughness values of the Mo/Si films prepared under 400 °C and 300 °C are shown in Table 3. It can be seen from Table 3 that under the same test temperature, the RMS roughness values of the as-implanted Mo/Si films were much larger than those of the corresponding non-implanted

Mo/Si films. It can be explained that Mo ion implantation resulted in rougher surface due to irradiation damage. As test temperature decreased to 300 °C, RMS roughness values of both the as-implanted Mo/Si film and non-implanted Mo/Si film decreased compare to their corresponding samples prepared under 400 °C.

The grain sizes of the Mo/Si films are listed in Table 3. It is clear that under the same test temperature, the grain sizes of the as-implanted Mo/Si films were much less than those of the corresponding non-implanted Mo/Si films. As test temperature decreased to 300 °C, the grain size of both the as-implanted Mo/Si films and non-implanted Mo/Si films increased compare to their corresponding samples prepared under 400 °C.
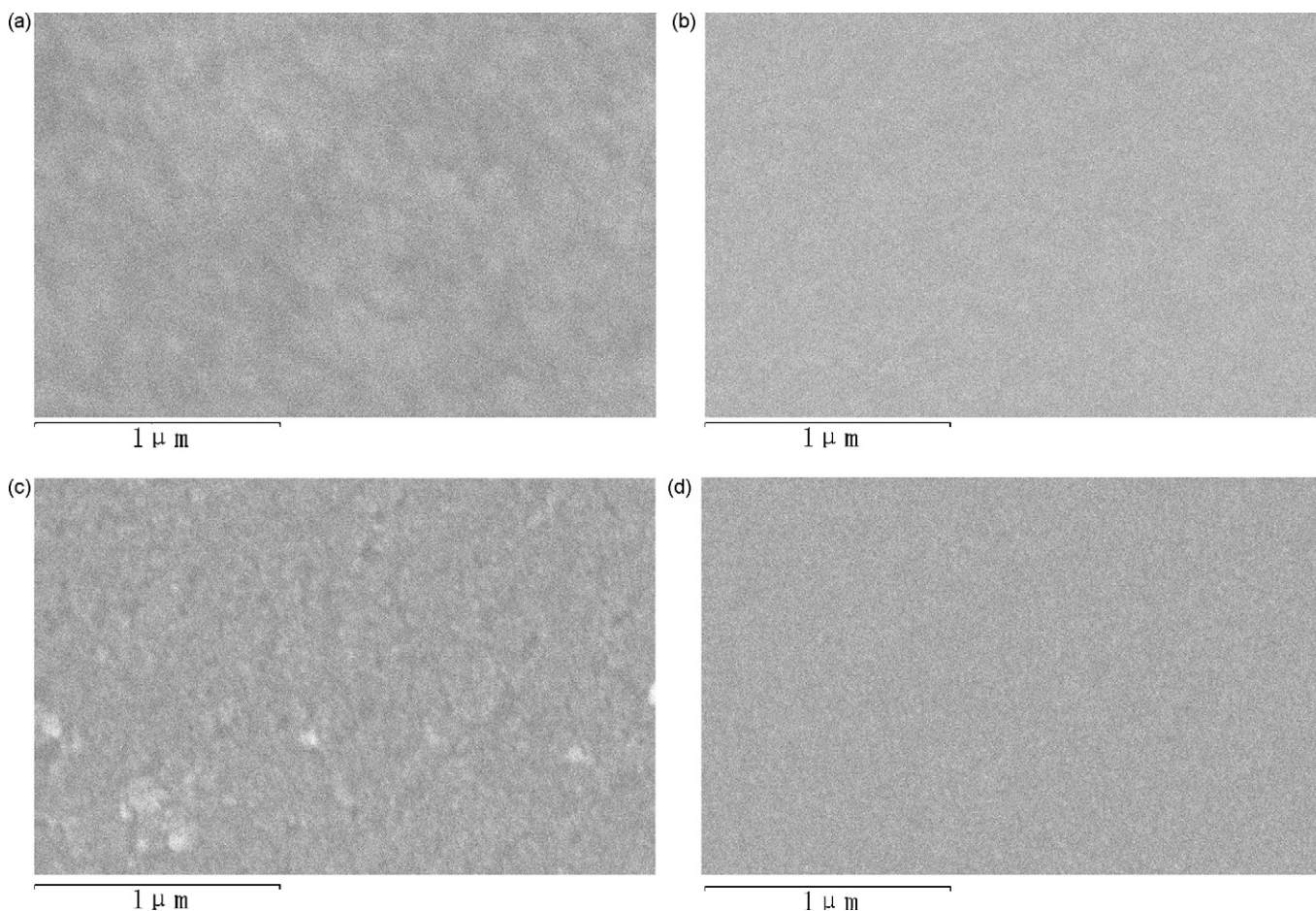


Fig. 2. SEM images of the Mo/Si films of (a) the sample A; (b) the sample a; (c) the sample B; (d) the sample b.

Table 2
Thickness of all the Mo/Si films

| | Sample no. | | | | | |
|---|---|---|---|---|---|---|
| | A | a | B | b | C | c |
| Thickness (nm) | 180 | 178 | 176 | 173 | 181 | 176 |

Table 3
RMS roughness and grain size of the Mo/Si films prepared under 400 and 300 °C

| | Sample no. | | | |
|---|---|---|---|---|
| | A | a | B | b |
| RMS roughness (nm) | 0.10 | 0.03 | 0.07 | 0.02 |
| Grain size (nm) | 111 | 213 | 163 | 234 |

## 3.2. XRD and XPS analysis

Fig. 4 shows the XRD spectra (Cu Kα irradiation, λ = 1.5418 Å) of the samples A, a, B, b, C and c. It can be seen from Fig. 4(a) that for the as-implanted Mo/Si sample prepared under the test temperature of 400 and 300 °C, only the phases of $MoSi_2$ and Si were found. As the test temperature decreased to 200 °C, it can be seen that the phase of $Mo_5Si_3$ was found besides the phases of $MoSi_2$, Si, and elementary Mo. Intensity of both the $Mo_5Si_3$ peak and $MoSi_2$ peak was much weak. It means that higher test temperature is good for formation of the $MoSi_2$ phase.
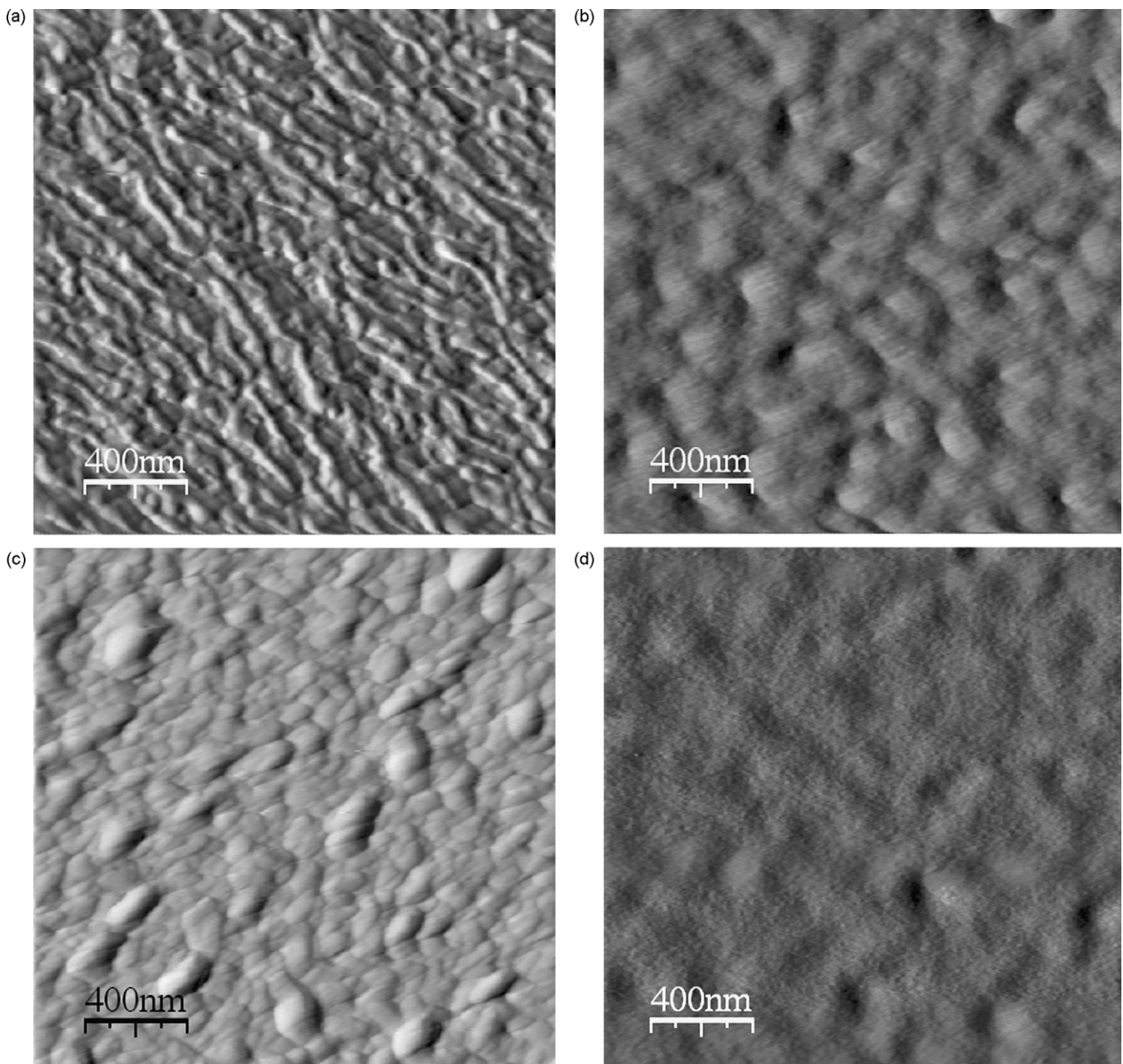


Fig. 3. AFM images of the Mo/Si films of (a) the sample A; (b) the sample a; (c) the sample B; (d) the sample b.
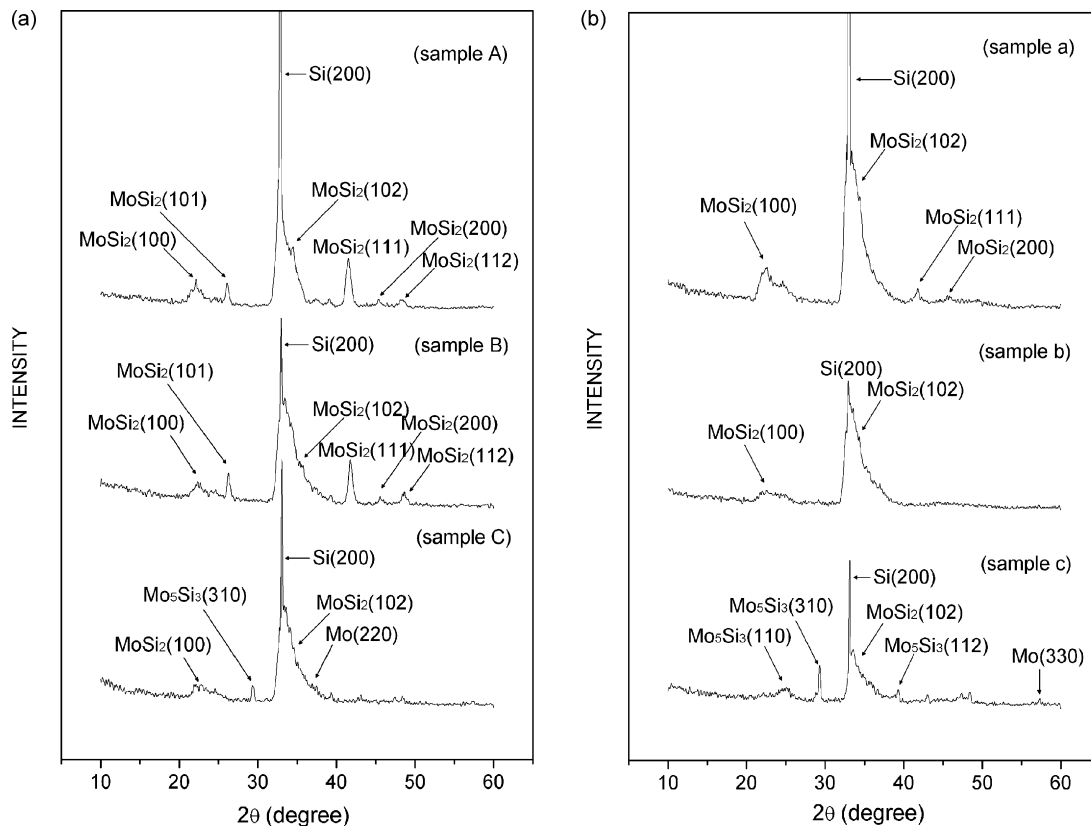
Fig. 4. (a) XRD spectra of the samples A–C; (b) XRD spectra of the samples a–c.

It can be seen from Fig. 4(b) that influence of the test temperature to the non-implanted Mo/Si films is the similar with one to the as-implanted Mo/Si films. Compare to both XRD spectra of the as-implanted and non-implanted Mo/Si films, it is obvious that Mo ion implantation is very useful for formation of the $MoSi_2$ phase. Some elementary Mo was also found in the Mo/Si film prepared at 200 °C.

Fig. 5(a and b) shows XPS spectra of the sample C and sample c, respectively. The relative amount of various components in the films was listed in Table 4. It is clear that the relative amount of $MoSi_2$ in the as-implanted Mo/Si film was more than one of $MoSi_2$ in the non-implanted Mo/Si film. The relative amount of $Mo_5Si_3$ in both the samples was less. It can also be observed that there was more elementary Mo left on surface of both the samples due to low test temperature. Tiny $MoO_2$ was traced to oxidation of the elementary Mo in both the Mo/Si films.

### 3.3. Sheet resistance of the Mo/Si films

The sheet resistance of the samples A, B, C, a, b, and c was measured by four-probe method, as shown in Table 5. It is clear that the as-implanted Mo/Si films were of a lower sheet resistance than corresponding non-implanted Mo/Si films. It means that Mo ion implantation enhanced formation of the $MoSi_2$ phase.

Also, it is clear from Table 5 that for both groups of the samples the sheet resistance of the Mo/Si film decreased as the test temperature decreased. It can be explained as following.
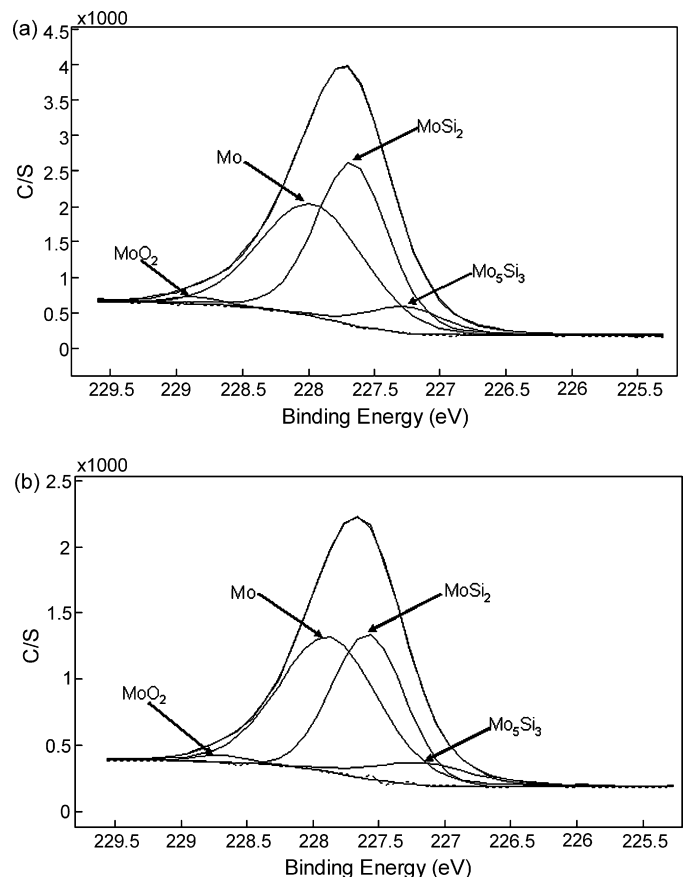


Fig. 5. (a) XPS spectrum of the sample C; (b) XPS spectrum of the sample c.

Table 4
XPS spectra of the sample C and sample c

| | Component | | | |
|---|---|---|---|---|
| | MoSi$_2$ | Mo$_5$Si$_3$ | Mo | MoO$_2$ |
| Area (%) | | | | |
| Sample C | 46.82 | 8.05 | 43.73 | 1.40 |
| Sample c | 38.37 | 8.47 | 51.84 | 1.32 |

The Mo atoms and Si atoms were sputtered from their targets, respectively, by incident Ar ions, and became energized atoms. As the test temperature decreased, Si atoms on surface of the Si substrate were much steady, and were much difficult to be sputtered away by the incident energized Mo atoms and Si atoms. Consequently, surface of the Mo/Si film prepared at lower test temperature should be smoother than one prepared at higher test temperature. It is well-known that sheet resistance of a conductive film on a smoother surface is lower than one on a rougher surface.

XRD and XPS results indicate that there was elementary Mo on surface of both the sample C and sample c. As a kind of metal, resistance of elementary Mo is very low. It is why the sheet resistances of the Mo/Si films prepared under 200 °C were lowest compare to their corresponding group of samples.

### 3.4. Nanohardness and modulus measurement

Two plots of the nanohardness as a function of indentation depth of both as-implanted and non-implanted Mo/Si films prepared under 400 °C are shown in Fig. 6. A series of indentations were made to depths ranging from 10 to 190 nm depending on the load. Each datum point represents an average value of five indentations. For the as-implanted sample, the nanohardness reached its maximum value of 26 GPa at 26 nm, as shown in Fig. 6(a). The nanohardness decreased rapidly with increasing depth of indentation in the near surface region, then, decreased smoothly to a value of more than 15 GPa. For the non-implanted sample, the nanohardness reached its maximum value of 17 GPa at 38 nm, as shown in Fig. 6(b), then, decreased smoothly to a value of around 15 GPa. In order to measure the "film-only" properties, a commonly used rule of thumb is to limit indentation depth to less than 10% of the thickness [15,16].

In this work, thickness of the Mo/Si films is around 180 nm. Accordingly, it is considered that the nanohardness value

Table 5
Sheet resistance of the Mo/Si films prepared under different test temperatures and implantation condition

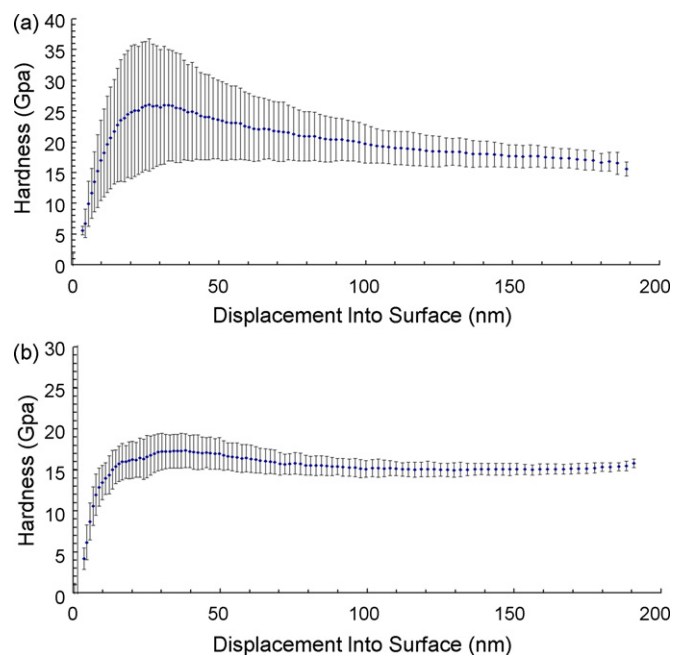| | Test temperature (°C) | | |
|---|---|---|---|
| | 400 | 300 | 200 |
| Mo/Si films with Mo ion implantation (Ω/□) | | | |
| Measurement value | 85 | 71 | 53 |
| Standard deviation | 7 | 1 | 7 |
| Mo/Si films without Mo ion implantation (Ω/□) | | | |
| Measurement value | 94 | 82 | 78 |
| Standard deviation | 13 | 5 | 4 |



Fig. 6. (a) Nanohardness of the as-implanted Mo/Si film prepared at 400 °C; (b) nanohardness of the non-implanted Mo/Si film prepared at 400 °C.

reflects Mo/Si film property only when the indentation depth is less than 18 nm. It is clear that the maximum nanohardness value of the as-implanted sample appeared at 26 nm, and one of the non-implanted sample appeared at 38 nm. Both of them were larger than 18 nm. It can be explained that the Mo/Si films were thin, and a compression deformation might occur during the nanohardness and modulus measurement.

Fig. 7 shows modulus of the as-implanted and non-implanted Mo/Si films on Si substrates. The results are also
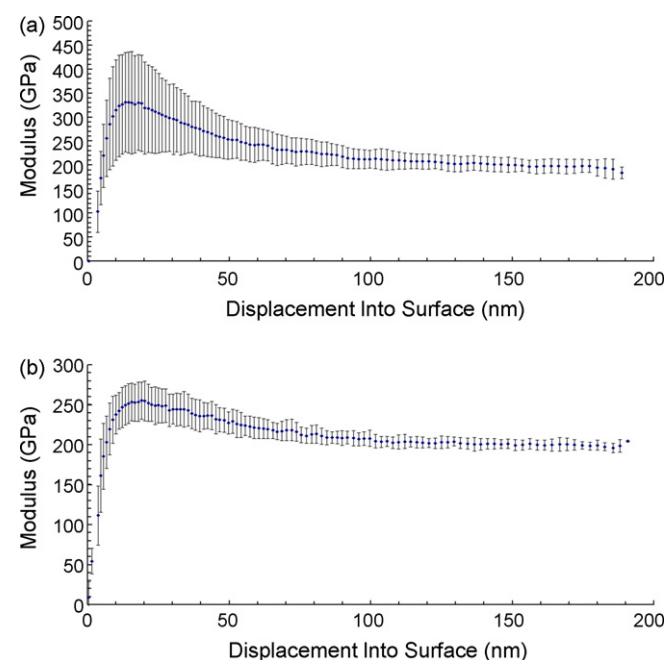


Fig. 7. (a) Modulus of the as-implanted Mo/Si film prepared at 400 °C; (b) modulus of the non-implanted Mo/Si film prepared at 400 °C.

plotted as a function of the indentation depth. Chudoba [17] suggests that it is very difficult to measure the correct modulus of some thin films, because the contact depths are required to be very small. Usually, the measured modulus reflects the composite information of both film and substrate. Liu found that the TiN film deposited on the $N^+$ implanted aluminum possessed greater ability to support loading and to resist plastic deformation than one deposited on non-implanted aluminum [18–22]. The composite modulus of the as-implanted sample is around 331 GPa at extremely small depths (13 nm), then, significantly decreased to about 213 GPa for the indentation depth of more than 100 nm. For the non-implanted sample, the modulus is around 255 GPa at a depth of 19 nm, then, decreased to a constant value of around 200 GPa with increasing depth of the indentation. With increasing depth of the indentation in the near surface region, both nanohardness and modulus of the as-implanted samples decreased faster than those of the non-implanted samples. The similar results were observed by Saha and Nix [23].

Compare Fig. 6 with Fig. 7, it is clear that nanohardness of the as-implanted sample reached its maximum value at 26 nm, while the modulus of the as-implanted sample reached its maximum value at 13 nm. It can be explained that the Mo/Si films were thin, and substrate effect had a larger influence to modulus value than to nanohardness value. That is why depth of the maximum value of nanohardness was deeper than one of the maximum value of modulus. Similarly, the nanohardness of the non-implanted sample reached its maximum value at 38 nm, while the modulus of the non-implanted sample reached its maximum value at 19 nm.

It is clear from Figs. 6 and 7 that nanohardness and modulus of the as-implanted Mo/Si film were larger than those of the corresponding non-implanted Mo/Si film. Also, at each displacement, values of nanohardness and modulus of the as-implanted Mo/Si film were of larger fluctuation than those of the corresponding non-implanted Mo/Si film. It is explained that surface of the as-implanted Mo/Si film was rougher than one of the non-implanted Mo/Si film.

## 4. Conclusion

The Mo/Si films were prepared by both IBAD deposition and MEVVA ion implantation technologies. Higher test temperature and Mo ion implantation are good for formation of $MoSi_2$ phase. The RMS roughness and grain size of the Mo/

Si films are closely related with preparation conditions. The sheet resistance of the as-implanted Mo/Si films was less than that of the corresponding non-implanted Mo/Si films.

The values of nanohardness and modulus of the Mo/Si films reached their maximum values at very thin depth near the surface, then, decreased with increasing depth of the indentation. The values of nanohardness and modulus of the Mo/Si films were affected greatly by test parameters.

## References

[1] M. Yu, J.Z. Zhang, D.X. Li, Q.L. Meng, W.Z. Li, Appl. Surf. Sci. 253 (2007) 3276.
[2] W.J. Park, S.C. Huh, K.Y. Lee, Int. J. Mod. Phys. B 20 (25–27) (2006) 3914.
[3] S. Suzuki, N. Hashimoto, T. Oyama, K. Suzuki, J. Adhesion Sci. Technol. 8 (1994) 261.
[4] E. Ando, S. Suzuki, J. Non-Cryst. Solids 218 (1997) 68.
[5] S. Suzuki, E. Ando, Thin Solid Films 340 (1999) 194.
[6] J.P. Gambino, E.G. Colgan, Mater. Chem. Phys. 52 (1998) 99.
[7] Q. Ma, M.K. Kang, China Molybdenum Ind. 21 (1997) 37.
[8] C.C. Chen, S.W. Chen, J. Mater. Sci. 32 (16) (1997) 4429.
[9] F. Loffler, Surf. Coat. Technol. 132 (2/3) (2000) 227.
[10] Y.F. Zhang, X.W. Zhang, Z.X. Ren, G.R. Han, Mater. Rev. 17 (2003) 40.
[11] L. Wang, Y.E. Zhao, F.L. Zhao, D.H. Chen, Chin. J. Lumin. 26 (2005) 636.
[12] M. Yu, J.Z. Zhang, D.X. Li, Q.L. Meng, W.Z. Li, Surf. Coat. Technol. 201 (2006) 1243.
[13] Y. Funada, Surf. Coat. Technol. 128 (2000) 308.
[14] J.F. Ziegler, J.P. Biersack, U. Littmark, The Stopping and Range of Ions in Matter, vol. 1, Pergamon Press, New York, 1985.
[15] W.C. Oliver, G.M. Pharr, J. Mater. Res. 7 (1992) 1564.
[16] N.G. Chechenin, J. Bottiger, J.P. Kroge, Thin Solid Films 261 (1995) 219.
[17] T. Chudoba, J. Mater. Res. 19 (2004) 301.
[18] Y.M. Liu, Surf. Coat. Technol. 200 (2006) 2672.
[19] S.B. Hu, J.P. Tu, Z. Mei, Surf. Coat. Technol. 141 (2001) 174.
[20] K. Dyrda, M. Sayer, Thin Solid Films 355/356 (1999) 277.
[21] R. Saha, W.D. Nix, Mater. Sci. Eng. A 319–321 (2001) 898.
[22] G.S. Kim, S.Y. Lee, J.H. Hahn, B.Y. Lee, J.G. Han, J.H. Lee, S.Y. Lee, Surf. Coat. Technol. 171 (2002) 83.
[23] R. Saha, W.D. Nix, Acta Mater. 50 (2002) 23.